IARJSET

ISSN (O) 2393-8021, ISSN (P) 2394-1588

International Advanced Research Journal in Science, Engineering and Technology

Impact Factor 8.066 ⁂ Peer-reviewed & Refereed journal ⁂ Vol. 13, Issue 7, July 2026

DOI: 10.17148/IARJSET.2026.13728

Finite Element Modelling of Reinforced Concrete and Advanced-Material Beam–Column Joints: A Review with a Gradient-Regularised Microplane Damage–Plasticity Case Study

Ankita Dhananjay Kulkarni[1], Dr. G.R. Gandhe[2]

Department of Civil Engineering, Deogiri Institute of Engineering and Management Studies, Chhatrapati Sambhajinagar (Affiliated to Dr. Babasaheb Ambedkar Technological University, Lonere, M.S.)[1,2]

Abstract: Reinforced concrete (RC) beam–column joints remain one of the most extensively investigated yet persistently challenging regions of framed structures, since they must transfer large, reversing shear forces through a compact, congested volume of concrete. This paper reviews the evolution of finite element (FE) approaches used to simulate beam–column joint behaviour, tracing the progression from classical pressure-sensitive plasticity models through continuum damage mechanics to coupled plasticity–damage and microplane formulations, culminating in the Gradient-Enhanced Plasticity-Damage Microplane (GPDM) model now implemented in ANSYS as the CPT215/CPT216 element families. Building on this theoretical foundation, the review synthesises recent experimental and numerical studies across three connection families: conventional reinforced concrete joints, joints constructed with Ultra-High-Performance Concrete (UHPC) and steel-fibre-reinforced concrete (SFRC), and steel or steel–concrete composite beam-to-column connections. To ground the review in a concrete demonstration, the paper presents a case study in which the GPDM model was applied to a benchmark exterior T-shaped RC joint (specimen JA-0, after Chalioris et al., 2008) under monotonic displacement-controlled loading. The FE model predicted a peak reaction force of 32.9 kN at 33.8 mm beam-tip displacement, within 4.4% of the experimentally reported peak, and reproduced the joint's characteristic elastic, hardening and post-peak softening phases, together with a shear-dominated failure mechanism consistent with the reported damage pattern. The synthesis identifies three converging research gaps — limited systematic mesh-sensitivity studies of gradient-regularised models for RC joints, an immature numerical toolkit for UHPC and SFRC connections, and under-exploited cross-fertilisation between steel/composite and RC joint research — and outlines directions for future work, including cyclic loading, bond-slip modelling and full-frame extensions.

Keywords: Beam–column joint; finite element analysis; ANSYS; microplane theory; damage plasticity; Ultra-High-Performance Concrete; seismic performance; mesh sensitivity.

1. INTRODUCTION

Reinforced concrete framed structures remain the dominant structural system for residential, commercial and infrastructural construction worldwide, owing to their strength, economy and constructional flexibility. Within such frames, the beam–column joint is the region where the internal forces of intersecting beams and columns must be resolved through a comparatively small volume of concrete. Under gravity loading this force-transfer mechanism behaves in a largely predictable manner; under seismic excitation, however, the joint core is subjected to rapidly reversing shear, diagonal strut action and bond-slip of longitudinal reinforcement, conditions under which inadequately detailed joints have repeatedly been implicated in building collapses, including in the Northridge (1994), Kocaeli (1999) and Izmir (1999) earthquakes.

Because full-scale cyclic testing of joints is expensive and cannot easily be varied across the many geometric and material parameters of interest, the finite element method (FEM) has become the principal complementary tool for investigating joint behaviour. The reliability of any such simulation, however, is governed almost entirely by the constitutive model used to represent concrete, a material whose response is characterised by tensile microcracking, compressive crushing, strain softening and pronounced tension–compression asymmetry. Early continuum models struggled to reproduce this behaviour without pathological mesh-dependent localisation in the post-peak regime, a limitation only recently overcome by gradient-regularised formulations that are now available in commercial FE codes.

DOI: 10.17148/IARJSET.2026.13728

This paper has two aims. First, it reviews how concrete constitutive modelling for beam–column joints has evolved, and synthesises recent literature across three related connection families — conventional RC joints, joints built with advanced high-performance concretes, and steel or composite beam-to-column connections — whose findings, though drawn from different material systems, share common threads relevant to joint design and simulation. Second, it presents a worked case study in which one of the most recent gradient-regularised constitutive models, the Gradient-Enhanced Plasticity-Damage Microplane (GPDM) model, is applied to a well-documented benchmark RC exterior joint and validated against experimental data, illustrating both the capability and the practical workflow of this modelling approach. The paper closes by drawing together the research gaps evident from the review and outlining directions for future investigation.

2. EVOLUTION OF CONCRETE CONSTITUTIVE MODELLING FOR JOINT SIMULATION

The development of constitutive models capable of representing concrete's nonlinear behaviour spans more than five decades. Classical plasticity models built on pressure-sensitive yield surfaces — the Drucker–Prager, Willam–Warnke and Ottosen criteria among them — were the first to capture rate-independent permanent deformation and confinement-dependent strength under predominantly compressive, monotonic loading. These models, however, cannot represent the progressive stiffness degradation that characterises cracked or cyclically loaded concrete, since plasticity theory alone has no mechanism for reducing elastic stiffness.

Continuum damage mechanics, introduced for concrete in the early 1980s, addressed this gap by defining scalar or tensorial internal variables that reduce the secant stiffness in proportion to the severity of microcracking. A purely scalar damage formulation, while computationally economical, cannot distinguish between tensile crack opening, compressive crushing and the partial stiffness recovery that occurs when cracks close under load reversal — a serious limitation for any joint expected to see cyclic seismic demand. Coupled plasticity–damage formulations subsequently became the accepted paradigm: Lee and Fenves (1998) split damage into tension and compression components to allow stiffness recovery on crack closure; Grassl and Jirásek (2006) reformulated plasticity in the effective (undamaged) stress space for improved algorithmic stability; and Poh and Swaddiwudhipong (2009) combined an implicit gradient approach with over-nonlocal weighting to fully regularise coupled plasticity–damage models, laying one of the theoretical foundations later used in the GPDM formulation.

A parallel line of development, microplane theory, establishes constitutive relations on planes of arbitrary orientation rather than through macroscopic stress and strain invariants, with the macroscopic stress tensor recovered by numerical integration over the unit sphere. This directional formulation naturally captures the anisotropy induced by cracking and frictional sliding. Carol and Bažant (1997) first embedded damage and plasticity within the microplane framework, and Zreid and Kaliske progressively regularised this model class between 2014 and 2018.

The Gradient-Enhanced Plasticity-Damage Microplane (GPDM) model of Zreid and Kaliske (2018) represents the current state of the art, unifying three previously separate developments within a single, commercially implemented framework: (i) a smooth, three-surface microplane cap yield function with C^1-continuity across the Drucker–Prager cone and the tension- and compression-cap regions, ensuring a well-posed return-mapping algorithm; (ii) a tension–compression damage split, weighted by the ratio of positive principal strains, that assigns separate exponential damage laws to tensile and compressive microplane strains and deactivates tensile damage under compression; and (iii) an over-nonlocal implicit gradient regularisation that introduces only two additional nodal degrees of freedom — homogenised nonlocal tension and compression strains — regardless of the number of microplanes used, achieving mesh-objective results without a prohibitive increase in system size. The model is implemented in ANSYS as the CPT215 (linear, eight-node) and CPT216 (quadratic, twenty-node) coupled-physics solid elements, with reinforcement typically represented by embedded REINF264 spar elements. This combination is the basis of the case study presented in Section 6.

3. THEMATIC REVIEW OF RECENT LITERATURE

The literature synthesised below is organised into three connection families that, while materially distinct, share a common concern with accurately predicting joint shear capacity, damage location and post-peak behaviour through finite element simulation.

3.1 Conventional Reinforced Concrete Beam–Column Joints

Experimental characterisation of RC joint behaviour dates to the 1960s, when Hanson and Connor first established the importance of transverse reinforcement within the joint core, and Paulay, Park and Priestley later formulated the diagonal strut-and-tie model that still underpins most seismic design provisions. Among more recent experimental programmes, Chalioris, Favvata and Karayannis (2008) tested twenty exterior beam–column joint specimens to evaluate crossed

DOI: 10.17148/IARJSET.2026.13728

inclined bars (X-bars) as joint shear reinforcement. Specimens with X-bars exhibited higher load capacity, improved hysteretic behaviour and damage that shifted away from the joint core into ductile beam plastic hinges; the combination of X-bars with conventional stirrups gave the best overall performance. The control specimen from this programme, containing no supplementary joint reinforcement, is used as the validation benchmark in Section 6 of this paper.

On the numerical side, Najafgholipour, Dehghan, Dooshabi and Niroomandi (2017) modelled RC joints governed by shear failure using the Concrete Damage Plasticity (CDP) framework, reporting good agreement with experimental load–displacement response, cracking patterns and ultimate strength, and confirming that a carefully calibrated CDP model can capture the brittle nature of joint shear failure. Drobnjak and Rakočević (2025) applied ANSYS to an RC exterior joint using a coupled damage-plasticity microplane formulation with REINF264 reinforcement elements, again achieving good agreement with experimental data; their systematic mesh-density study found that prismatic elements with triangular bases converge faster than hexahedral elements at equivalent densities, and that element sizes below roughly 35 mm are needed for reliable post-peak predictions — a finding that directly motivates mesh-sensitivity investigation of gradient-regularised models such as GPDM. Their analysis, however, was confined to monotonic loading and did not address hysteretic behaviour, stiffness degradation or bond-slip, leaving cyclic joint simulation an open problem. Ahmed et al. subsequently applied the GPDM model itself to an RC joint specimen, obtaining close agreement with experimental load–displacement curves and establishing the reference ANSYS simulation against which further GPDM-based joint studies, including the present case study, can be benchmarked.

3.2 Ultra-High-Performance and Fibre-Reinforced Concrete Joints

A parallel strand of research has explored advanced concrete materials as a route to overcoming the intrinsic limitations of conventional RC joint construction. Ultra-High-Performance Concrete (UHPC), characterised by compressive strengths exceeding 150 MPa, tensile strengths of 5–15 MPa and dense steel-fibre reinforcement, has been investigated for both cast-in-place and precast connections. Ma, Deng and Yang (2021) studied internal precast beam–column connections cast in UHPC, finding that the material substantially enhances joint shear strength, relocates damage away from the joint core into the adjacent beam or column, and reduces reinforcement congestion relative to conventional cast-in-place joints; their proposed shear-capacity model outperformed standard RC code equations. Su, Tan and Lu (2026) reported comparable benefits for exterior reinforced-UHPC joints, observing suppressed cracking and plastic hinge relocation into the beams — the strong-column, weak-beam mechanism sought by modern seismic codes — and noted that existing RC design equations, which do not account for UHPC's fibre-bridging action, significantly underestimate joint capacity.

Wang, Yang, Zhou and Jiang (2025) extended this line of work to prefabricated columns using a hybrid reinforcement system combining GFRP bars, a steel spiral-confined concrete core and UHPC connections, aimed at resolving the trade-off between the corrosion resistance of GFRP and its inherently brittle behaviour. Cyclic testing showed that UHPC connections improved load transfer efficiency and seismic performance while allowing shorter lap-splice lengths, with damage again relocated away from the connection. In precast segmental bridge construction, where keyed dry joints between segments must transfer substantial shear, Zheng, Cui, Xuan, Ma, Li and Li (2023) examined UHPC splicing joints under direct shear, finding that lateral compressive stress markedly improves performance, that double-key configurations outperform single-key joints, and that existing AASHTO and European code provisions do not accurately predict UHPC joint strength. Li, Wang, Ma, Zhao, Wang, Lv and Ye (2025) combined finite element analysis with an analytical model to study steel-fibre-reinforced concrete (SFRC) single-keyed dry joints, showing that fibre content and lateral confining pressure are the dominant parameters governing shear capacity, that failure initiates through stress concentration at the shear-key root, and that a calibrated FE model can support practical parametric optimisation of key geometry and mix design. Taken together, these studies indicate that while UHPC and SFRC deliver clear performance gains, the numerical tools needed to simulate their fibre-bridging and confinement-sensitive behaviour without mesh dependence are still comparatively immature — a gap the gradient-regularised microplane framework is well positioned to address.

3.3 Steel and Composite Beam-to-Column Connections

Although constructed from a different material system, steel and steel–concrete composite connections have generated findings that inform RC joint interpretation, particularly regarding axial–flexure interaction, stress concentration and connection detailing. El-Khoriby, Sakr, Khalifa and Eladly (2017) developed simplified two- and three-dimensional shell finite element models of steel beam-to-column connections subjected to combined axial force and cyclic bending, demonstrating that axial force significantly influences stiffness, strength and hysteretic response and should not be neglected in seismic design, while keeping computational cost low enough for practical parametric studies. Mashaly, El-Heweity, Abou-Elfath and Osman (2011) used finite element analysis to evaluate stress distribution, rotational capacity

IARJSET ISSN (O) 2393-8021, ISSN (P) 2394-1588

International Advanced Research Journal in Science, Engineering and Technology

Impact Factor 8.066 ⁒ Peer-reviewed & Refereed journal ⁒ Vol. 13, Issue 7, July 2026

DOI: 10.17148/IARJSET.2026.13728

and energy dissipation in steel joints under cyclic loading, confirming that connection detailing strongly governs achievable ductility and that FE predictions agree well with experimental observations.

Xuesen, Yujie and Quanxi (2025) modelled high-strength steel cover-plate beam-to-column joints, finding that cover plates substantially improve stiffness, strength and moment resistance, with stress concentrations concentrated near welded regions, and proposed a design method for practical application. Zhao, Shi, Chen and Xiao (2021) investigated welded haunches as a seismic retrofit for older steel joints, showing that haunches increase load capacity, relocate plastic hinges away from the column face, and improve energy dissipation — conceptually paralleling the damage-relocation strategies observed for X-bar-reinforced and UHPC RC joints in Sections 3.1 and 3.2. At the composite interface, Liu, Li and Liew (2026) developed multi-linear and bi-linear moment–rotation hinge models for composite beam–column connections under sagging and hogging moments for progressive-collapse analysis, while Giżejowski, Barcewicz and Salah (2010) built a three-dimensional nonlinear FE model of semi-rigid composite steel–concrete end-plate joints with relatively thin end plates, showing that composite action from the concrete slab substantially enhances strength and rotational capacity. Finally, Sabat and Kundu (2023) examined flexural–torsional interaction in steel beam sections using ANSYS Workbench, finding that eccentric loading, which induces combined bending and torsion, is markedly more critical than concentric loading, and that hollow circular and rectangular sections resist torsion more effectively than open I-sections — a reminder that section geometry and load eccentricity, not just material constitutive behaviour, materially affect connection performance.

4. RELEVANT DESIGN CODE PROVISIONS

Numerical studies of beam–column joints are typically framed against, and validated with reference to, national and international design codes. IS 456:2000 establishes the basic limit-state design framework for RC members, including anchorage length, development length and reinforcement ratio requirements relevant to force transfer at the joint. IS 13920:2016 is the principal Indian code for ductile detailing of RC structures under seismic loading, specifying transverse joint-core reinforcement, confinement and anchorage requirements consistent with the strong-column, weak-beam philosophy. IS 1893 (Part 1):2016 provides the seismic force calculation procedures — zoning, response reduction factors and design spectra — that define the loading demand a joint must resist. Internationally, ACI 318-19 offers a comparable framework, with explicit provisions for joint shear strength, reinforcement anchorage and ductile detailing under the same strong-column, weak-beam principle. As noted in Section 3.2, several UHPC and SFRC studies report that these RC-oriented code equations systematically underestimate the shear capacity of high-performance-concrete joints, since none of the provisions account for fibre-bridging contributions — underscoring a code-development gap that parallels the numerical modelling gap identified in this review.

5. SYNTHESIS OF RESEARCH GAPS

Three convergent gaps emerge from the literature reviewed above. First, although the GPDM model represents the most theoretically complete, commercially available gradient-regularised constitutive model for concrete, its systematic application to RC beam–column joints — including mesh-sensitivity behaviour across multiple element types and sizes, and detailed post-processing of internal damage and plasticity variables — remains limited in the published record; most available studies (e.g. Drobnjak and Rakočević, 2025) instead employ the earlier coupled damage-plasticity microplane model. Second, while UHPC and SFRC connections have been shown experimentally to deliver substantial performance gains, the numerical tools needed to simulate their fibre-bridging and confinement-sensitive behaviour efficiently and without mesh dependence are still being established; the gradient-regularisation and microplane kinematics underlying GPDM make it a strong candidate for this purpose, but its application to high-performance-concrete joints has not yet been demonstrated in the literature reviewed here. Third, steel and composite connection studies have identified behavioural features — axial–flexure interaction, stress concentration near welds, and damage relocation through retrofit or reinforcement detailing — that have clear analogues in RC joint behaviour and whose treatment demands the same high-fidelity constitutive modelling; these findings, while drawn from a different material system, usefully inform interpretation of RC joint simulation results. The case study presented next addresses the first of these gaps directly, providing a demonstration of GPDM-based simulation and validation for a benchmark RC exterior joint.

6. CASE STUDY: GPDM-BASED SIMULATION OF AN EXTERIOR RC BEAM–COLUMN JOINT

To ground the preceding review in a concrete demonstration, this section summarises a three-dimensional nonlinear finite element analysis carried out in ANSYS Workbench, applying the GPDM constitutive model to the control specimen (JA-0) of the exterior T-shaped beam–column joint tested experimentally by Chalioris, Favvata and Karayannis (2008).

IARJSET
ISSN (O) 2393-8021, ISSN (P) 2394-1588
International Advanced Research Journal in Science, Engineering and Technology
Impact Factor 8.066 ⁜ Peer-reviewed & Refereed journal ⁜ Vol. 13, Issue 7, July 2026
DOI: 10.17148/IARJSET.2026.13728

Specimen JA-0 contains no stirrups and no crossed inclined bars within the joint region, making it the baseline case for assessing joint shear behaviour in the absence of supplementary shear reinforcement.

6.1 Modelling Approach

The two-thirds-scale specimen comprises a 1800 mm column (300 × 200 mm cross-section) and an 1100 mm beam (200 × 300 mm cross-section), reinforced with 4Ø14 mm + 2Ø10 mm column bars and 4Ø12 mm top and bottom beam bars, with concrete compressive strength f′c = 34.0 MPa and steel yield strength fy = 500 MPa. Concrete was discretised with eight-node CPT215 solid elements employing the GPDM constitutive law, with a structured hexahedral mesh (approximately 25 mm element size) refined in the joint core where high stress gradients and damage were anticipated. Reinforcement was represented using REINF264 spar elements embedded within the concrete mesh, assigned a bilinear isotropic hardening model with a tangent modulus of 1000 MPa. The column base was fully fixed, a constant axial load of 9480 N was applied at the column top, and an 80 mm monotonic displacement was imposed at the beam tip under displacement control, matching the experimental protocol. The nonlinear equations were solved using a Newton–Raphson scheme with automatic time stepping and large-deflection effects enabled; the analysis completed 461 cumulative iterations over 87 substeps without divergence, indicating stable numerical performance even through the post-peak softening regime.

6.2 Force–Displacement Response and Validation

Figure 1 presents the predicted reaction force at the beam support against the applied beam-end displacement. Three phases are evident. Up to approximately 8 mm displacement the response is linear elastic, with no plastic strain recorded in either concrete or reinforcement. Between 8 mm and roughly 34 mm the response hardens nonlinearly as concrete micro-cracking (initiating as early as 0.8 mm) and, from 8.6 mm onward, reinforcement yielding both progress, reaching a peak reaction force of 32.914 kN at 33.80 mm displacement. Beyond this point the joint exhibits pronounced post-peak softening, with the reaction force falling to 14.951 kN at 80 mm — a 54.6% reduction from peak — consistent with brittle joint shear failure in the absence of transverse joint reinforcement.

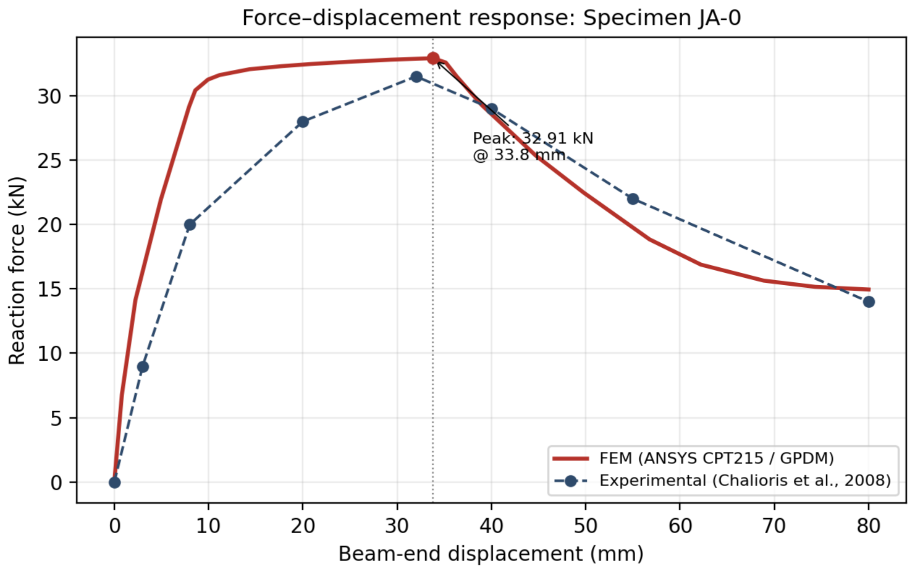

Fig 1. Predicted force–displacement response of specimen JA-0 (ANSYS GPDM/CPT215) compared with the experimental envelope reported by Chalioris et al. (2008).

The numerical peak of 32.9 kN at 33.8 mm compares with an experimentally reported peak of approximately 31.5 kN at approximately 32 mm displacement, a difference of about 4.4%, which lies within the accepted tolerance for nonlinear finite element simulation of concrete structures. The predicted initial stiffness (1.90 kN/mm) is likewise close to the experimental value (1.82 kN/mm, +4.4%), and the qualitative failure mode — diagonal cracking and progressive concrete crushing within the joint core, accompanied by yielding of the beam longitudinal bars at the joint face — matches the joint-shear failure (Damage Mode A) reported experimentally for this specimen.

IARJSET ISSN (O) 2393-8021, ISSN (P) 2394-1588

International Advanced Research Journal in Science, Engineering and Technology

Impact Factor 8.066 ⁘ Peer-reviewed & Refereed journal ⁘ Vol. 13, Issue 7, July 2026

DOI: 10.17148/IARJSET.2026.13728

6.3 Damage evolution: rebar and concrete plastic strain

Figure 2 tracks the evolution of equivalent plastic strain separately in the reinforcement and the concrete. Rebar plastic strain initiates at 8.6 mm displacement and increases through the hardening phase, but stabilises at a maximum of 0.0331 mm/mm beyond 35 mm, indicating that the longitudinal bars reach their plastic capacity well before the end of loading. Concrete plastic strain, by contrast, initiates earlier (0.8 mm) and continues to grow throughout the entire loading history, reaching 0.0568 mm/mm at 80 mm — more than double the terminal rebar strain. This divergence is diagnostic: it demonstrates that the pronounced post-peak strength loss observed in Figure 1 is governed almost entirely by progressive concrete damage and joint-core crushing rather than by further reinforcement yielding, a distinction that a purely plasticity-based or non-regularised damage model would be less able to resolve cleanly.

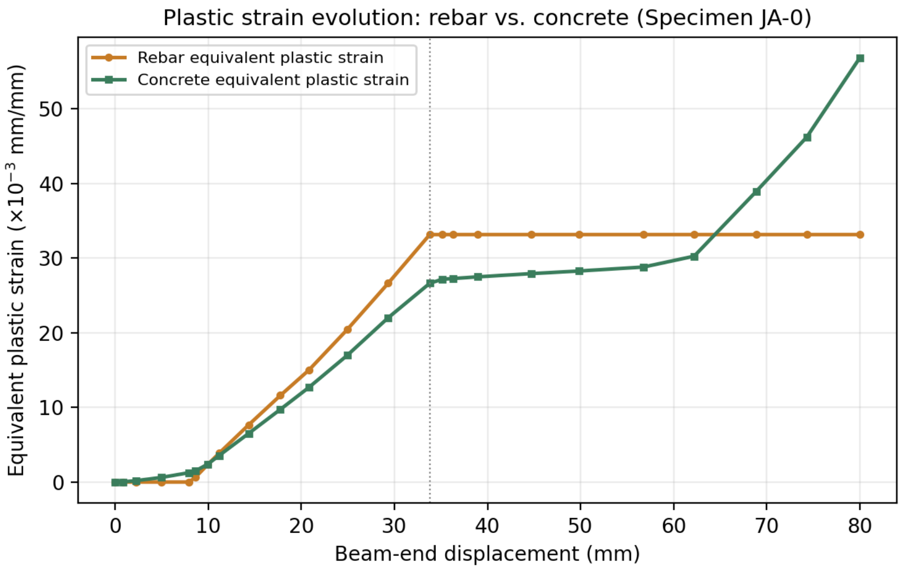

Fig 2. Evolution of equivalent plastic strain in the reinforcement and in the concrete, showing rebar strain saturation at 35 mm versus continued concrete damage growth to 80 mm.

6.4 Summary of case study findings

The maximum rebar equivalent stress reached 503 MPa at peak load, marginally exceeding the nominal 500 MPa yield strength through the strain-hardening branch of the bilinear steel model, before falling to 387.3 MPa (a 23% reduction) at 80 mm as the damaged joint could no longer sustain the same level of force transfer through the beam bars. The maximum total deformation of the model (88.997 mm) exceeded the 80 mm displacement imposed at the beam tip, the difference reflecting additional joint-panel shear distortion and local concrete crushing at the joint corners not captured by the applied boundary displacement alone. Collectively, these results demonstrate that the GPDM model, implemented through CPT215 elements, reproduces both the global load–displacement response and the internal damage mechanisms of a benchmark RC exterior joint with good quantitative accuracy and a physically consistent failure narrative, while remaining numerically stable through severe post-peak softening — the regime in which conventional smeared-cracking formulations (e.g. the legacy SOLID65 element) are most prone to convergence difficulty.

7. DISCUSSION

Read together, the reviewed literature and the case study point to several cross-cutting observations. First, mesh-objective, gradient-regularised constitutive models are no longer a purely academic refinement: the mesh-sensitivity findings of Drobnjak and Rakočević (2025) and the stable, convergent post-peak response obtained with GPDM in Section 6 both indicate that regularisation is a practical prerequisite for trustworthy post-peak joint simulation, not merely a theoretical nicety. Second, a recurring theme across materially distinct connection types — X-bar-reinforced RC joints, UHPC and SFRC connections, and haunch-retrofitted or cover-plated steel joints — is that improved connections do not primarily increase peak capacity alone; they relocate damage away from the joint core into more ductile, replaceable regions such as the beam. This shared strategy suggests that FE tools capable of resolving where damage concentrates, such as the plastic-strain field demonstrated in Section 6.3, are of comparable practical value to those that merely predict peak load. Third, the repeated observation that existing RC-oriented design equations underestimate the capacity of UHPC and SFRC joints indicates that validated finite element models currently serve not only as research tools but as a

DOI: 10.17148/IARJSET.2026.13728

practical bridge between advanced-material experimentation and code development, pending the eventual revision of design provisions to account for fibre-bridging and confinement effects.

8. CONCLUSIONS AND FUTURE RESEARCH DIRECTIONS

This review has traced the evolution of concrete constitutive modelling for beam–column joint simulation from classical plasticity through continuum damage mechanics to the gradient-regularised microplane models now available in commercial finite element software, and has synthesised recent findings across conventional RC, UHPC/SFRC, and steel/composite connection research. A case study application of the GPDM model to a benchmark exterior RC joint demonstrated close agreement with experimental load–displacement data (within 4.4% at peak load) and a physically consistent damage narrative, distinguishing rebar-governed hardening from concrete-governed post-peak softening, while maintaining stable numerical convergence throughout severe post-peak softening.

Building on the gaps identified in Section 5, several directions merit future investigation: extension of the current monotonic GPDM model to cyclic, reversed-displacement loading to capture hysteretic behaviour, stiffness and strength degradation, and energy dissipation, validated against cyclic experimental data; incorporation of explicit bond-slip interface elements between reinforcement and surrounding concrete, particularly for bars passing through the joint panel; a systematic parametric study of joint aspect ratio, axial load level, transverse reinforcement ratio and concrete grade using the validated model as a platform; application of the same gradient-regularised microplane approach to UHPC and FRP-retrofitted joints, where high tensile strength and confinement substantially alter the failure mechanism; independent calibration of the GPDM gradient-regularisation parameters directly from standard tension and compression test data, rather than adoption of literature values; and extension from single-joint to full-frame analysis to investigate how joint deformation and failure influence global structural response under pushover or dynamic loading.

REFERENCES

[1]. Ahmed, A. et al. (2019). Application of the gradient-regularised coupled damage–plasticity microplane model to a reinforced concrete beam–column joint. ANSYS Inc. technical validation report.
[2]. Carol, I., & Bažant, Z. P. (1997). Damage and plasticity in microplane theory. International Journal of Solids and Structures, 34(29), 3807–3835.
[3]. Chalioris, C. E., Favvata, M. J., & Karayannis, C. G. (2008). Reinforced concrete beam–column joints with crossed inclined bars under cyclic deformations. Earthquake Engineering & Structural Dynamics, 37(6), 881–897.
[4]. Drobnjak, I., & Rakočević, M. (2025). Analysis of reinforced concrete beam-column joint in ANSYS software.
[5]. El-Khoriby, S., Sakr, M. A., Khalifa, T. M., & Eladly, M. M. (2017). Modelling and behaviour of beam-to-column connections under axial force and cyclic bending. Journal of Constructional Steel Research, 129, 171–184.
[6]. Giżejowski, M. A., Barcewicz, W., & Salah, W. (2010). Finite element modelling of the behaviour of a certain class of composite steel-concrete beam-to-column joints. Archives of Civil Engineering, 56(1), 27–52.
[7]. Grassl, P., & Jirásek, M. (2006). Damage-plastic model for concrete failure. International Journal of Solids and Structures, 43(22–23), 7166–7196.
[8]. Lee, J., & Fenves, G. L. (1998). Plastic-damage model for cyclic loading of concrete structures. Journal of Engineering Mechanics, 124(8), 892–900.
[9]. Li, Y., Wang, R., Ma, Y., Zhao, G., Wang, S., Lv, J., & Ye, B. (2025). Direct shear behaviour of steel fiber-reinforced concrete single-keyed dry joints: Finite element analysis and calculation model. Structures, 81, 110362.
[10]. Liu, H., Li, S., & Liew, J. R. (2026). Moment hinge model for composite beam-column connections under sagging and hogging conditions for progressive collapse analysis. Engineering Structures, 362, 122979.
[11]. Ma, F., Deng, M., & Yang, Y. (2021). Experimental study on internal precast beam–column ultra-high-performance concrete connection and shear capacity of its joint. Journal of Building Engineering, 44, 103204.
[12]. Mashaly, E., El-Heweity, M., Abou-Elfath, H., & Osman, M. (2011). Finite element analysis of beam-to-column joints in steel frames under cyclic loading. Alexandria Engineering Journal, 50(1), 91–104.
[13]. Najafgholipour, M. A., Dehghan, S. M., Dooshabi, A., & Niroomandi, A. (2017). Finite element analysis of reinforced concrete beam-column connections with governing joint shear failure mode. Latin American Journal of Solids and Structures, 14(7), 1200–1225.
[14]. Poh, L. H., & Swaddiwudhipong, S. (2009). Over-nonlocal gradient enhanced plastic-damage model for concrete. International Journal of Solids and Structures, 46(24), 4369–4378.
[15]. Sabat, L., & Kundu, C. K. (2023). Flexural-torsional analysis of steel beam structures using ANSYS. Materials Today: Proceedings.
[16]. Su, J., Tan, X., & Lu, F. (2026). Seismic behaviour of exterior beam–column joints in reinforced ultra-high-performance concrete frames: An experimental and theoretical study. Journal of Building Engineering, 116288.

DOI: 10.17148/IARJSET.2026.13728

[17]. Wang, T., Yang, F., Zhou, Z., & Jiang, R. (2025). Experimental study on seismic performance of prefabricated UHPC-connected GFRP/steel hybrid reinforced columns. Structures, 77, 109069.
[18]. Xuesen, C., Yujie, Z., & Quanxi, Y. (2025). Finite element analysis and design method of high-strength steel cover-plate beam-to-column joints. Structures, 79, 109634.
[19]. Zhao, H., Shi, G., Chen, X., & Xiao, T. (2021). Finite element analysis and design of retrofitted beam-to-column joints with welded haunches. Journal of Constructional Steel Research, 186, 106924.
[20]. Zheng, H., Cui, C., Xuan, S., Ma, X., Li, Z., & Li, Y. (2023). Experimental study on direct shear performance of prefabricated splicing joints of ultra-high-performance concrete. Case Studies in Construction Materials, 18, e01771.
[21]. Zreid, I., & Kaliske, M. (2018). A gradient-regularized coupled damage–plasticity microplane model for concrete-like materials. International Journal of Solids and Structures.
[22]. IS 456:2000. Plain and Reinforced Concrete – Code of Practice. Bureau of Indian Standards, New Delhi.
[23]. IS 13920:2016. Ductile Design and Detailing of Reinforced Concrete Structures Subjected to Seismic Forces – Code of Practice. Bureau of Indian Standards, New Delhi.
[24]. IS 1893 (Part 1):2016. Criteria for Earthquake Resistant Design of Structures. Bureau of Indian Standards, New Delhi.
[25]. ACI 318-19. Building Code Requirements for Structural Concrete and Commentary. American Concrete Institute, Farmington Hills, MI.

